Supplement of

Energetics of monsoons and deserts: role of surface albedo vs water vapor feedback

Chetankumar Jalihal[1,2] and Uwe Mikolajewicz[1]

[1]Max Planck Institute for Meteorology, Hamburg
[2]Indian Institute of Technology Hyderabad

Correspondence: Chetankumar Jalihal (chetankumar.jalihal@mpimet.mpg.de)

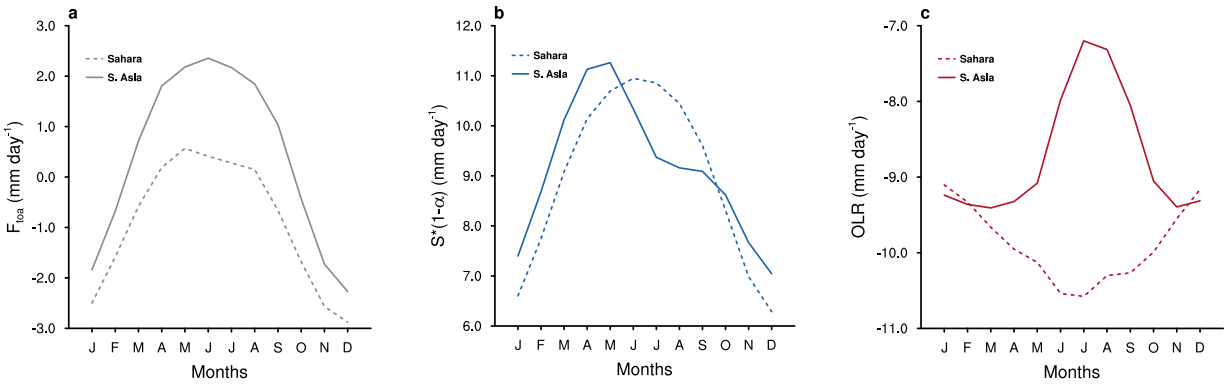

Figure 1. Seasonal cycle of F_{toa} and its components. The time series of (**a**) F_{toa}, (**b**) Net shortwave at the top of atmosphere, and (**c**) outgoing longwave radiation from ERA-5 climatology (based on 1981-2020). The solid line represents the area average over the domain (70°E-105°E and 15°N-30°N), while the dashed line shows the area average over the domain (0°E-30°E and 15°N-30°N).

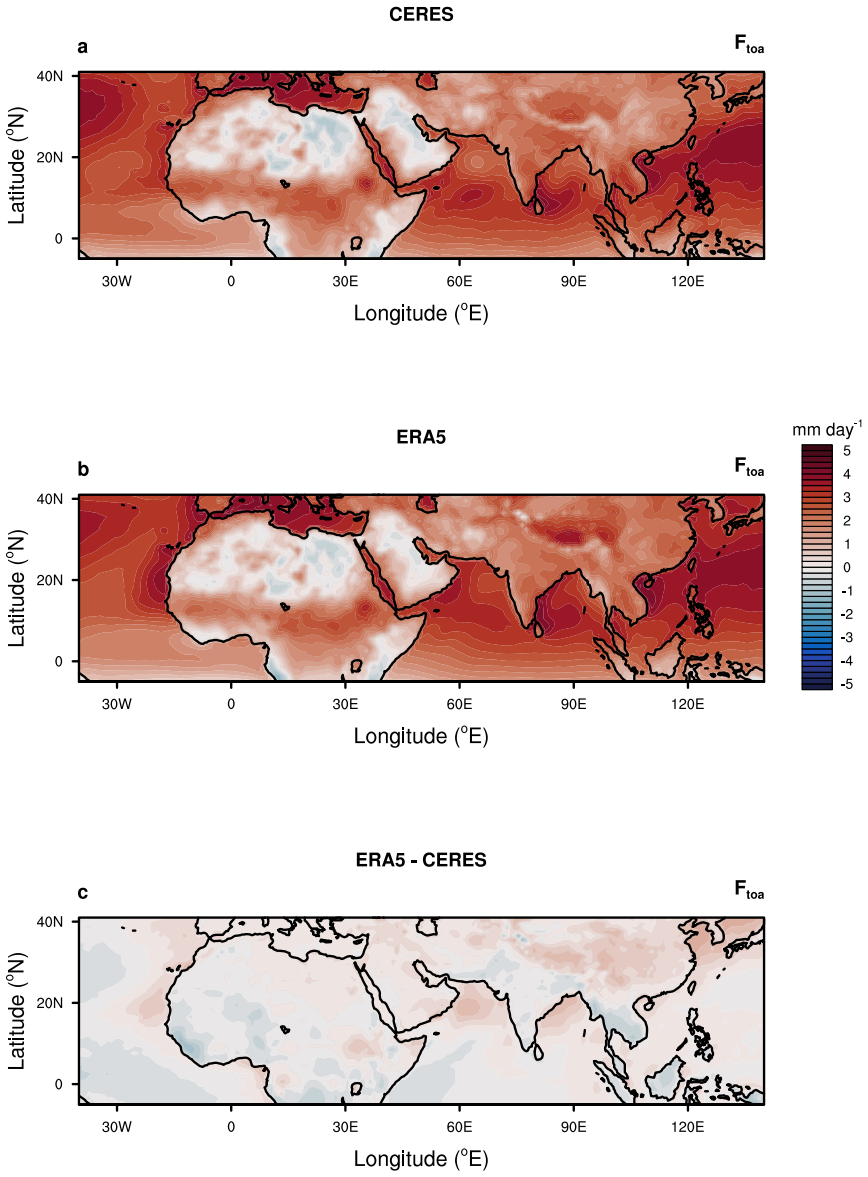

Figure 2. F_{toa} from ERA-5 and CERES Spatial maps of JJA climatological F_{toa} obtained from (**a**) CERES, (**b**) ERA-5, and (**c**) difference between ERA-5 and CERES. The ERA-5 climatology spans from 1981 to 2020, while the CERES climatology is based on the period from 2005 to 2015.

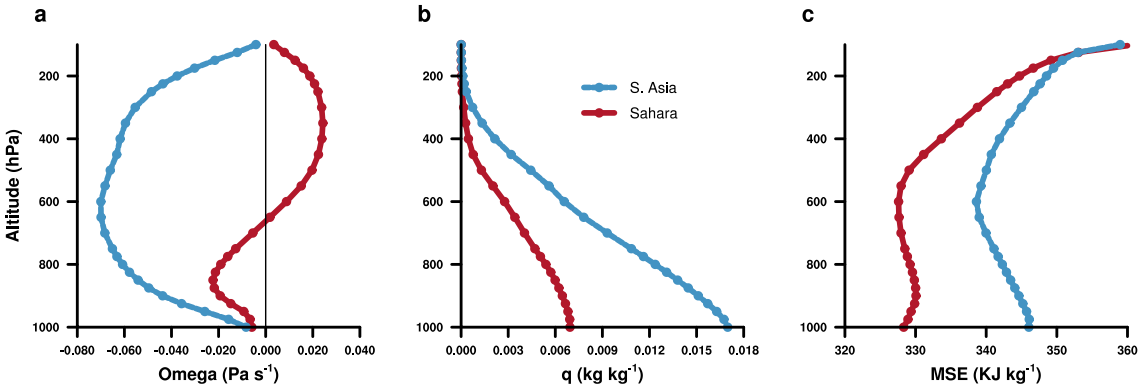

Figure 3. Vertical profiles over monsoons and deserts. Vertical profile of (**a**) vertical pressure velocity, (**b**), specific humidity, and (**c**) moist-static energy. The area-averaged parameters for South Asia (70°E-105°E; 15°N-30°N) and the Sahara (0°E-30°E and 15°N-30°N) are shown in blue and red, respectively. The Jun-Jul-Aug climatology from 1981 to 2020 is obtained from ERA-5.

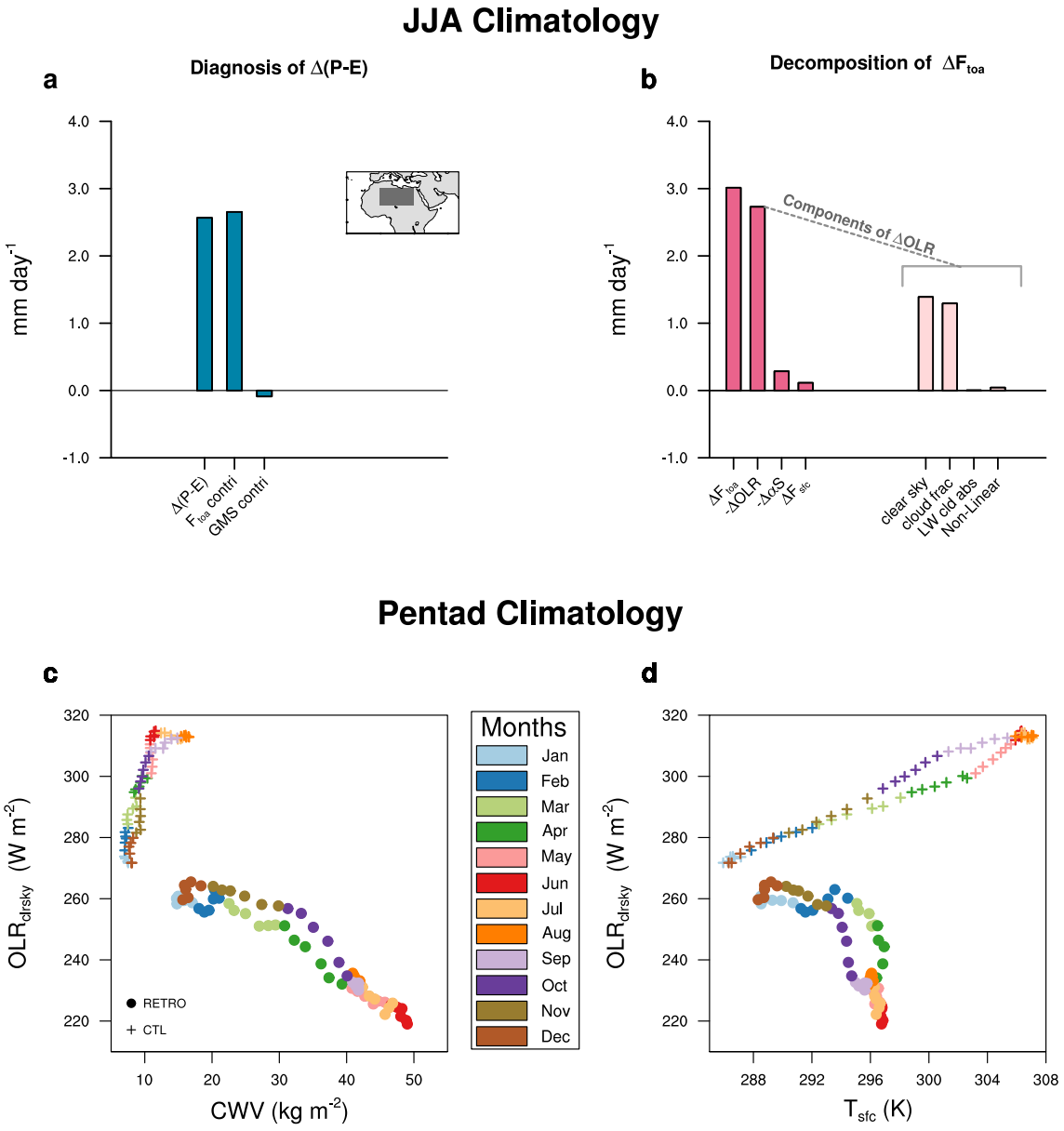

Figure 4. Diagnosis of change in moisture convergence between RETRO and CTL. Bar graph of (**a**) the difference in Precipitation minus Evaporation (P-E) between the RETRO and CTL Sahara, contribution of F_{toa}, and GMS, & (**b**) the difference in F_{toa} and its components. The change in OLR is further decomposed into changes due to clear sky OLR, changes in cloud area fraction, the longwave cloud absorption, and non-linear term (see methods). (**c**) & (**d**) shows a scatter of clear sky OLR with column-integrated water vapor and surface temperature, respectively. JJA climatology of the last 100 years is considered for this analysis. The region selected for this analysis is shown in the inset map: 0°E-30°E and 15°N-30°N; land-only grid points.

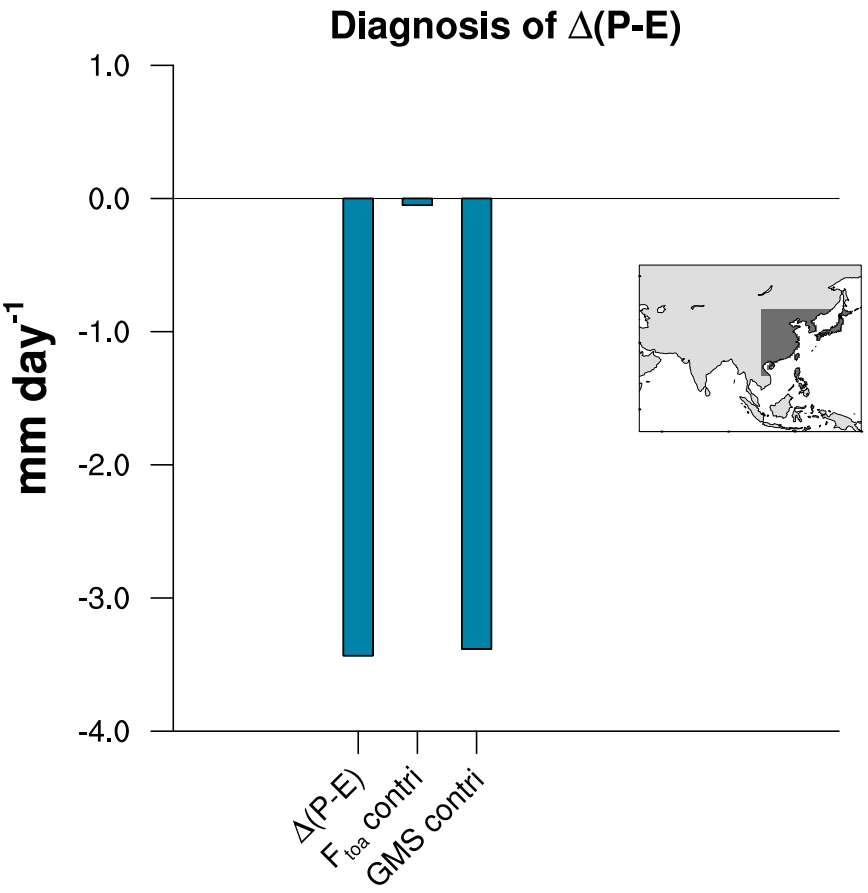

Figure 5. Diagnosis of moisture convergence over South East Asia. Bar graph of change in (Precipitation - Evaporation; P-E), contribution of F_{toa}, and GMS. The changes between Jun-Jul-Aug climatology between RETRO and the CTL over the domain (105°E-150°E and 15°N-45°N; shown in grey shading in the inset map), is considered for this analysis.

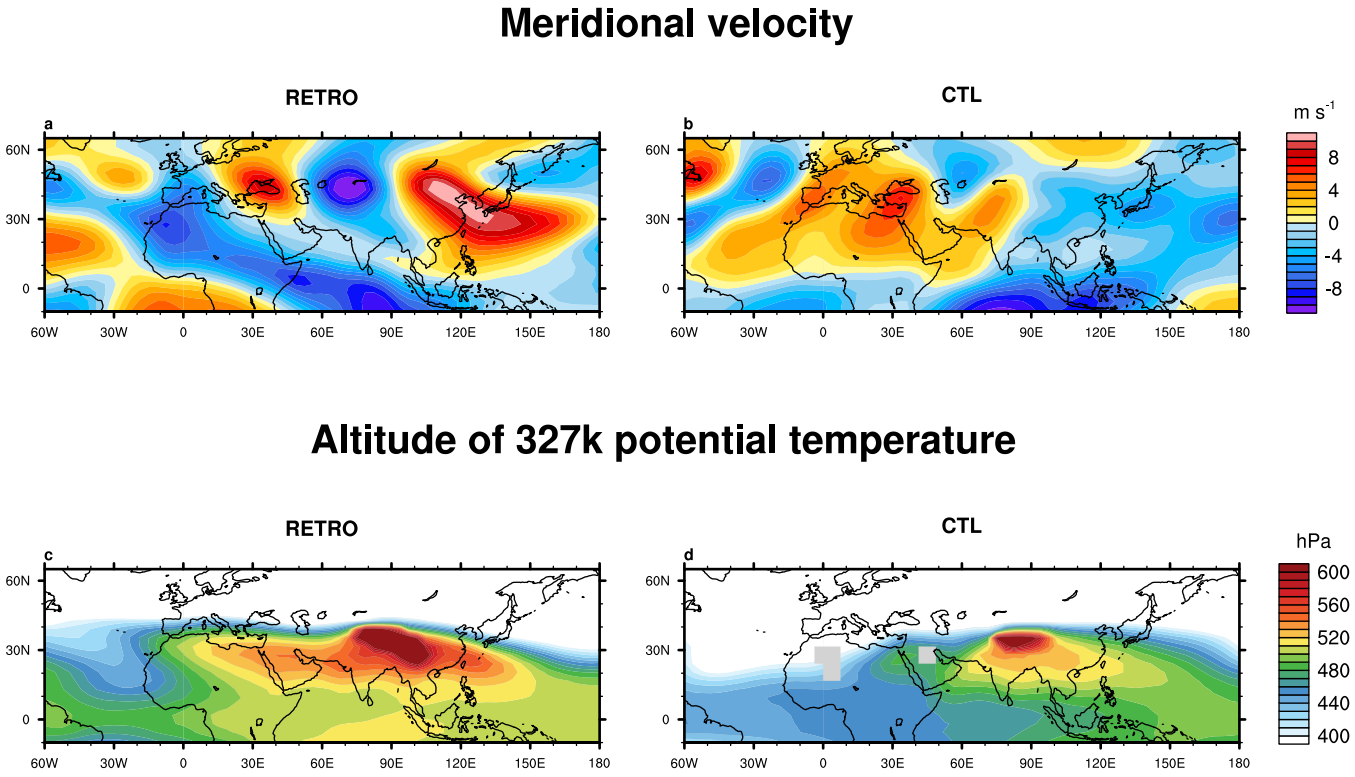

Figure 6. Meridional velocity and 327K potential temperature. Spatial maps of (**a**) & (**b**) meridional velocity and (**c**) & (**d**) the altitude of 327K potential temperature. (**a**) & (**c**) are from the RETRO simulation, and (**b**) & (**d**) depict the CTL simulation. Jun-Jul-Aug climatology of the last 100-yrs of the simulation are used for these plots.

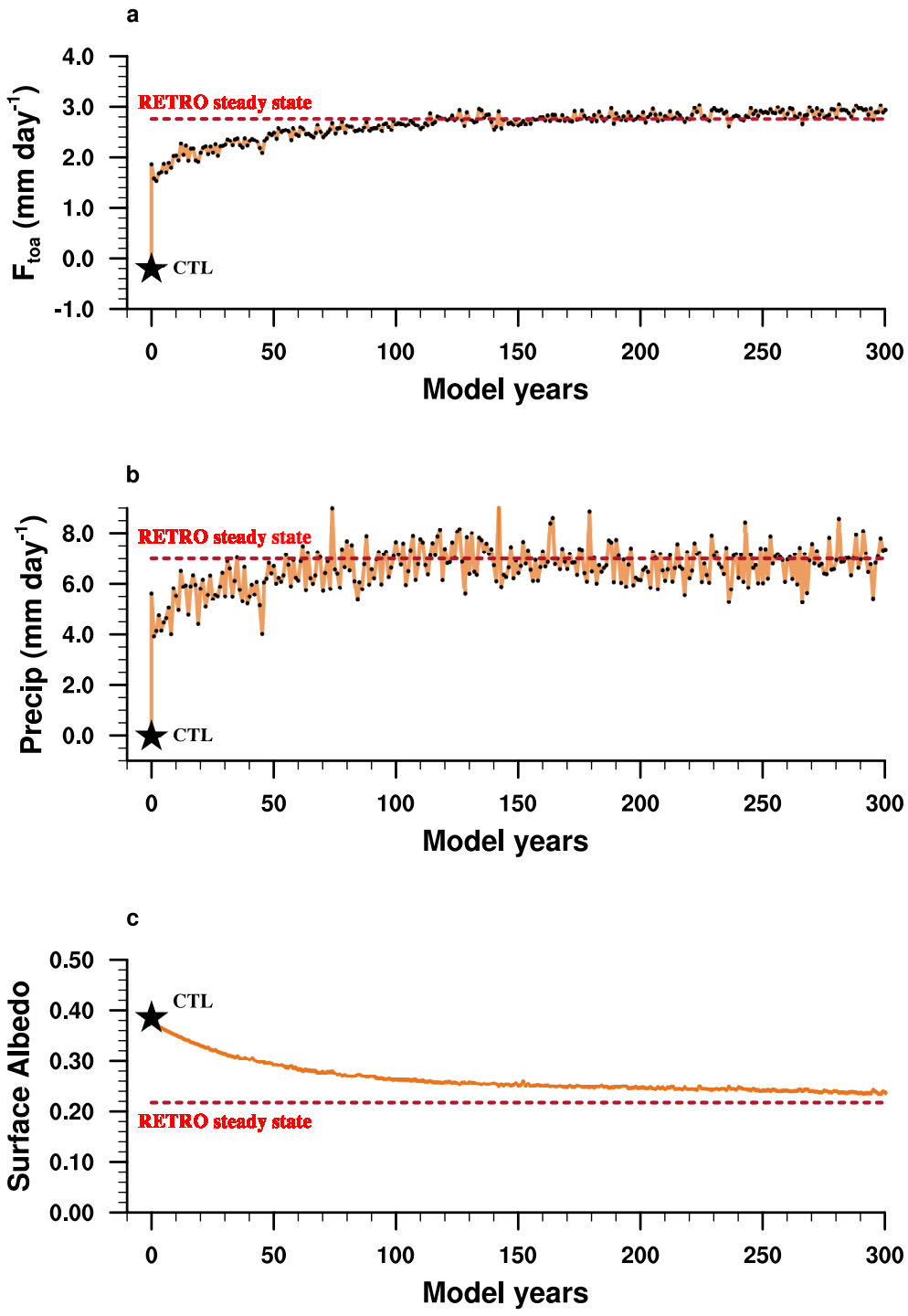

Figure 7. Temporal evolution of F_{toa}, precipitation, and surface albedo during spin-up. The time series of (**a**) F_{toa}, (**b**) precipitation, and (**c**) surface albedo, area averaged over the domain (0°E-30°E and 15°N-30°N). The orange line depicts the transients in the RETRO, and the red dashed line is the steady-state value. The filled star shows the steady-state value in the CTL.

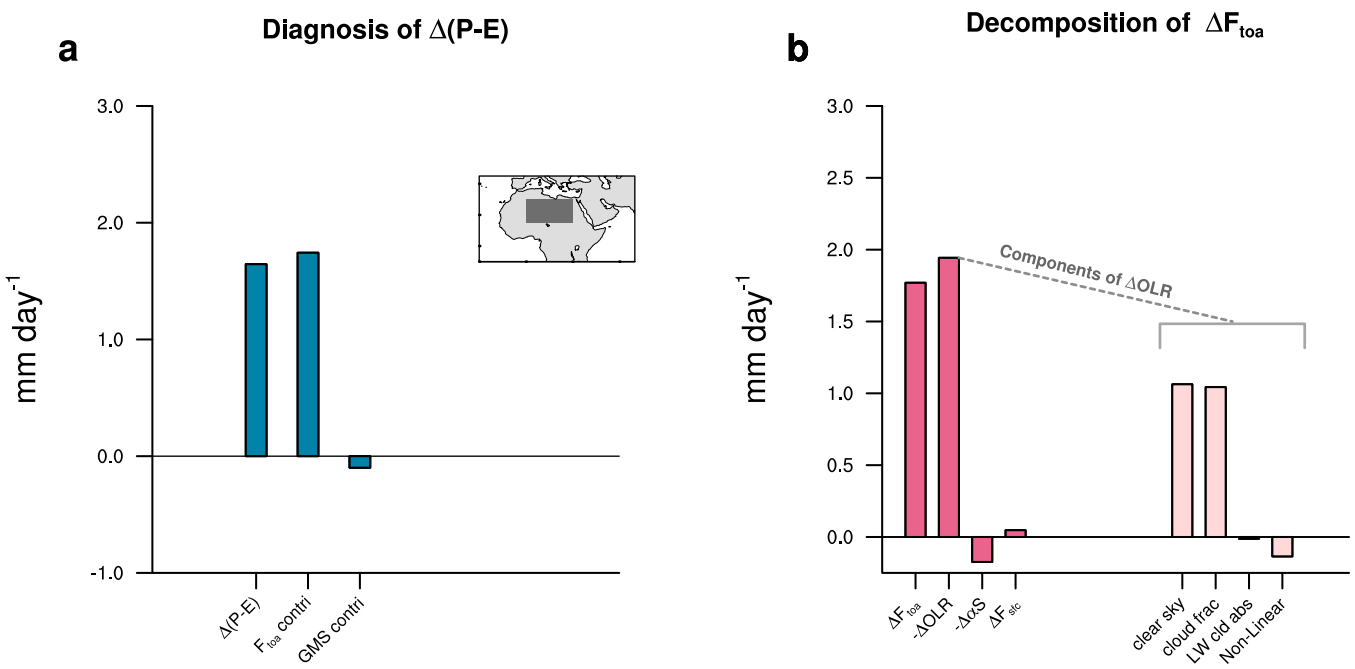

Figure 8. Diagnosis of change in moisture convergence during the first year of simulation. Bar graph of (**a**) change in (Precipitation - Evaporation; P-E), contribution of F_{toa}, and GMS, & (**b**) the change in F_{toa} and its components (see methods). The changes between Jun-Jul-Aug average of the first year of simulation from the RETRO and Jun-Jul-Aug climatology from the CTL over the domain (0°E-30°E and 15°N-30°N shown in grey shading in the inset map), is considered for this analysis. The change in OLR is further decomposed into changes due to clear sky OLR, changes in cloud area fraction, the longwave cloud absorption, and non-linear term (see methods).

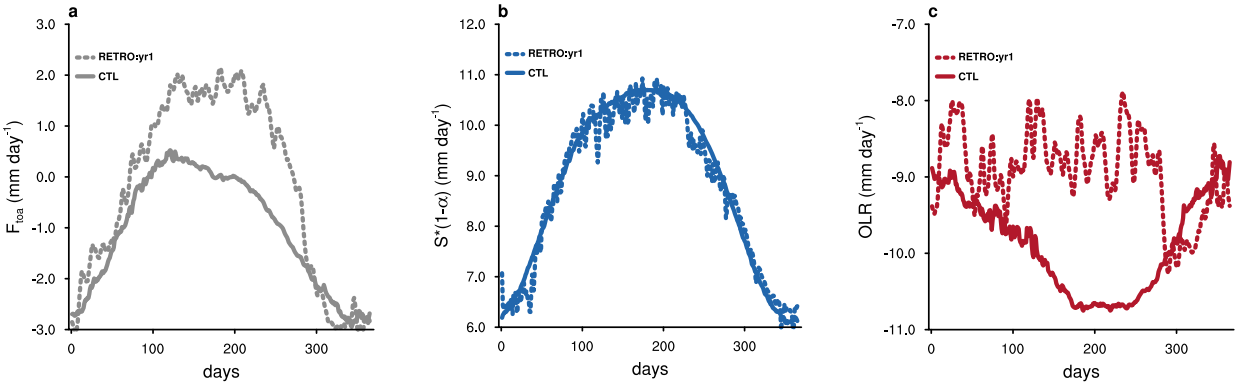

Figure 9. Seasonal cycle of F_{toa} and its components. The time series of (**a**) F_{toa}, (**b**) Net shortwave at the top of atmosphere, and (**c**) outgoing longwave radiation area averaged over the domain (0°E-30°E and 15°N-30°N). The solid line represents the steady-state from CTL, and the dashed line represents the first year of simulation from RETRO. Area average of the daily data is taken. Positive values are the energy gained by the atmosphere.